



University of the  
West of England

Eveness, J., Kiely, J., Hawkins, P., Wraith, P. and Luxton, R. W. (2009) Evaluation of paramagnetic particles for use in a resonant coil magnetometer based magneto-immunoassay. *Sensors & Actuators: B. Chemical*, 139 (2). pp. 538-542. ISSN 0925-4005 Available from: <http://eprints.uwe.ac.uk/80>

We recommend you cite the published version.

The publisher's URL is:

<http://dx.doi.org/10.1016/j.snb.2009.03.078>

Refereed: Yes

(no note)

Disclaimer

UWE has obtained warranties from all depositors as to their title in the material deposited and as to their right to deposit such material.

UWE makes no representation or warranties of commercial utility, title, or fitness for a particular purpose or any other warranty, express or implied in respect of any material deposited.

UWE makes no representation that the use of the materials will not infringe any patent, copyright, trademark or other property or proprietary rights.

UWE accepts no liability for any infringement of intellectual property rights in any material deposited but will remove such material from public view pending investigation in the event of an allegation of any such infringement.

PLEASE SCROLL DOWN FOR TEXT.

# **Evaluation of Paramagnetic Particles for use in a Resonant Coil Magnetometer based Magneto-Immunoassay**

John Eveness, Janice Kiely, Peter Hawkins, Patrick Wraith, Richard Luxton

Institute of Bio-sensing Technology  
University of the West of England, Bristol  
Coldharbour Lane  
Bristol BS16 1QY  
UK

## **Abstract**

This paper describes work that formed a part of an investigation to increase the detection sensitivity of a magneto-immunoassay. The study involved the characterisation of paramagnetic particles (PMPs) from a range of manufacturers in order to determine parameters that influence the assay sensitivity. Magnetisation curves were produced for each PMP type using a vibrating sample magnetometer. A resonant coil magnetometer which incorporated a planar, spiral coil integrated with a phase locked loop based detector was used to investigate the effect of PMP number and mass on the resonant frequency of the coil. In order to compare performance in an assay using a resonant coil magnetometer, the sensitivity for a monolayer of particles was evaluated. The results enabled the identification of parameters that were critical to achieving maximum sensitivity and, of the particles studied, the 0.75  $\mu$ m diameter PMPs demonstrated the greatest sensitivity in the resonant coil magnetometer.

*Keywords:*

*Magneto-Immunoassay; Paramagnetic particles; Resonant Coil Magnetometer.*

## 1. Introduction

An immunoassay is a well established technique for determining the quantity of target antigen within a test sample. The principal concept of this technique is the highly specific and sensitive interactions between antigens and their antibodies [1]. A label or marker must be added in order to quantify the interaction between antigen and antibody.

In the medical field paramagnetic particles (PMPs) have widespread application in blood detoxification, biochemical separations, drug delivery, dynamic DNA hybridization, nucleic acid separation, and are also used as MRI contrast agents [2,3]. The structure and properties of PMPs are dependent on the materials and methods of fabrication. They are commonly manufactured with a polymer coating, encapsulating an inner iron-oxide core. The coating protects the target molecule from exposure to iron, prevents particle aggregation and can be used to immobilise biological molecules that interact with a sample, providing a coated solid phase. PMPs are used as labels in immunoassays, in order to quantify the binding between a target antigen and the corresponding antibody, creating a magneto-immunoassay (MIA). In comparison with other types of labels, such as radioisotopes, enzymes, chemiluminescent [4] molecules, PMP labels have a number of advantages. They are low cost, stable, non-toxic, re-usable, can be stored indefinitely and be easily localised and manipulated by a magnetic field [5].

A MIA can be used to quantify any analyte for which a pair of antibodies is available. For example, a MIA has been used to detect Troponin I at the clinically relevant level of 0.5 ng/ml [5] and CKMB with a detection limit of 2ng/ml [6]. Both Troponin I and CKMB are biomedical markers of myocardical infarction, ie a heart attack.

A diagrammatic representation of a MIA that utilises a resonant coil detector is shown in figure 1. The key steps to perform a MIA are as follows: The polymer coatings, typically polystyrene, of the PMPs are modified to introduce carboxyl or amino groups which allow the covalent coupling of proteins to the surface using a coupling chemistry such as 1-ethyl-3-(3-dimethylaminopropyl)carbodiimide Hydrochloride / N-hydroxysuccinimide. An antibody against the target is then conjugated onto the PMPs and a second antibody is applied to the reaction surface in the reaction vessel; in the majority of cases a monoclonal antibody coats the PMP and a polyclonal antibody is immobilised on the reaction surface. The clinical sample containing target molecules to be detected, and PMPs coated are then added to a phosphate buffer solution in a reaction vessel. External magnetic fields are used to pull the PMPs onto an antibody coated reaction surface. The PMPs are captured by the specific interaction between the detecting antibody on the PMP, the antigen and the antibody, which is immobilised on the reaction surface. Subsequently, the external magnetic fields are used to remove unbound PMPs from the reaction. The PMPs that are bound to the reaction surface

perturb the magnetic field of a sensing coil, thus the amount of antigen present in a sample is quantified by a variation in the coil inductance. A sandwich assay format is shown in figure 1; however PMPs can be used as a label in both a sandwich and competitive immunoassay [7]. The detection sensitivity of the MIA is dependent on the affinity of the antibodies to the target antigen, the coil parameters, stability of the detection circuitry and, importantly, PMP label characteristics.

This paper describes an analytical approach to predict the PMP type, from a range of commercially available samples that would give optimum detection sensitivity in a MIA. In addition, in this paper the PMP properties that influence the sensitivity when used in a MIA, in conjunction with a resonant coil magnetometer (RCM), are identified.

## **2. Experimental**

In this work a number of commercially available PMPs were compared to determine the optimum label for use within a MIA. PMPs from a selection of manufacturers, which varied in structure and method of manufacture, were contrasted. Table 1 shows the PMP diameter and the percentage of magnetic material in the PMP as quoted in the manufactures' data sheets for each of the PMPs studied. The numbers of PMPs per mL in the stock solutions which were determined using a microscope and haemocytometer are also shown.

### **2.1 Mass susceptibility measurements**

In preparation for determining magnetisation curves for each PMP type, 5  $\mu$ l samples of PMPs were dried on to a filter paper and placed within a measurement tube; the mass of particles per sample volume was calculated. A Quantum Design vibrating sample magnetometer (VSM) was used to perform magnetic measurements on 5  $\mu$ L samples within the range of  $\pm 2500$  Oe at 300 K.

### **2.2 Resonant coil magnetometer**

In a MIA the change in coil inductance, which is a function of the number of bound PMPs, is determined using a resonant coil magnetometer (RCM). In this work the RCM used a phase locked loop based detection circuit, as shown in figure 2, to measure relative changes in resonant frequency caused by variation of sensing coil inductance (L). A voltage controlled oscillator (VCO) supplied the LC circuit. A phase detector sensed the phase difference of the signal across resistance, R, and, after filtering, produced a DC error signal that is fed back to the VCO. The negative feedback error signal changed the output frequency of the VCO until there is no difference in phase between  $V_s$  and  $V_o$ . Thus, the frequency of the signal from the VCO is locked onto the resonant frequency of the tuned LC circuit. When the sensing coil inductance (L) changed due to PMPs being adjacent to the coil, the VCO output frequency

changed accordingly. Richardson [8] has demonstrated that, for a helical coil design, the relationship between frequency output and the number of PMPs in the reaction surface adjacent to the coil is linear.

Figure 3 shows the experimental arrangement ie 35 MHz phase locked loop detection circuit, five 4 turn sensing coils on an interface PCB, electromagnet with focusing studs and a reaction vessel. The vessel consisted of resin walls affixed to a 0.15mm thick glass slide which is positioned directly over the sensing coils. The glass base of the vessel formed the reaction surfaces. Five coils and associated reaction surfaces allowed multiple measurements to be performed in parallel. The electromagnet and focusing stud were designed to produce an external DC magnetic field to manipulate PMPs onto the reaction region adjacent to the sensing coil.

To determine the relationship between output frequency and quantity of PMPs, the following experimental procedure was adopted. Firstly 100  $\mu\text{L}$  of PBS buffer solution was added to the reaction vessel. Secondly, the electromagnet was switch on, and finally a volume of PMPs was positioned directly onto the reaction surface; volumes of 0.5  $\mu\text{L}$ , 1  $\mu\text{L}$ , 2  $\mu\text{L}$ , 4  $\mu\text{L}$ , 8  $\mu\text{L}$  were used. The frequency response was logged throughout the complete experimental period and  $\Delta f$  was determined by equation (1).

$$\Delta = f_1 - f_2 \quad (1)$$

Where,  $f_1$  is the average frequency of the reference coil over 100 seconds and  $f_2$  represents the average frequency of the sensing coil over 100 seconds.

### 3. Theoretical properties of a monolayer of PMPs.

During a magneto-immunoassay measurement, following binding of PMPs on the reaction surface, the magnet field is altered to remove unbound particles from the surface. Consequently, the maximum number of PMPs that can be detected represent a monolayer across the detection region adjacent to the sensing coil.

For monolayer coverage, the number ( $N_{pmp}$ ) can be determined from the area of the coil ( $A_{coil}$ ) and the cross sectional area of a paramagnetic particle ( $A_{pmp}$ ), assuming hexagonal packing and the number of particles around the circumference of the coil being very small compared with the total number (equation (2)).

$$N_{pmp} \approx 0.9 \cdot \frac{A_{coil}}{A_{pmp}} \quad (2)$$

For the test system used in this study the area of each coil ( $A_{coil}$ ) was 4.91  $\text{mm}^2$ .

To provide a comparison between the responses of the RCM to the various PMPs a parameter termed the mass susceptibility of a monolayer ( $\chi_{monolayer}$ ) with units of emu/Oe was used (equation (3)). This parameter is dependent on the mass of a monolayer of PMPs ( $m_{monolayer}$ ); the percentage of magnetic material in a PMP ( $\%_{mag. material}$ ) and its mass susceptibility of a PMP ( $\chi_m$ ).

$$\chi_{monolayer} = n_{monolayer} \cdot \%_{mag. material} \cdot \chi_m \quad (3)$$

Since the mass of a monolayer is merely the mass of a single PMP multiplied by the number in a monolayer, the susceptibility can be rewritten as shown in equation (4).

$$\chi_{monolayer} = n_{pmp} \cdot N_{pmp} \cdot \%_{mag. material} \cdot \chi_m \quad (4)$$

Further from equation (2), the expression for susceptibility of a monolayer can be rewritten to include the diameter of the PMP, as shown in equation (5).

$$\chi_{monolayer} \approx n_{pmp} \cdot 0.9 \cdot \left( \frac{A_{coil}}{A_{pmp}} \right) \%_{mag. material} \cdot \chi_m \quad (5)$$

## 4. Results and discussion

### 4.1 Magnetic Particle Characterisation.

Figure 4 shows the magnetisation curves for the range of PMP types and for a pure magnetite sample. Each plot shows the characteristic linear region and saturation point. The susceptibility is given by the gradient of the magnetisation versus field strength plot and is maximum for each material at the zero field point. The mass susceptibility as determined using the VSM for each type of PMP can be related not only to the susceptibility of the magnetic material within the sample, but also the % magnetic material content of the PMP, as 1g of sample of PMPs includes both magnetic material and encapsulating polymer. The magnetite demonstrates the largest susceptibility value as well as the highest saturation point. The values of mass susceptibility measured at zero field and saturation magnetisation for the range of PMPs chosen for this study are given in table 1. Table 1 illustrates that, in general, the smallest PMPs have the greatest percentage magnetic material content and record the highest saturation magnetisation.

### 4.2 Particle evaluation using resonant coil magnetometer

Figure 5 shows the frequency shift ( $\Delta f$ ) versus PMP sample mass ( $\mu g$ ) measured using the RCM for the five PMP types which were the focus of this study. For each sample mass three replicate tests were performed ( $n=3$ ) and standard errors are shown in figure 5. For each of the plots, at low sample mass values the relationship between the frequency shift and the

calculated mass is approximately linear, as an increasing mass of PMP causes greater perturbation of the field of the coil and hence a larger change in resonant frequency. Figure 5 shows that for larger values of sample mass the plots begin to show a saturation effect. Saturation in this case is a physical phenomenon where a film of particles completely coats the detection region of the coil and consequently further increases in mass of PMPs does not have such a significant effect on the coil. At very high concentrations, during measurement, the spot of PMPs could be observed to spread beyond the detection region, i.e. the area of the sensing coil. The result of this experiment shows that for a given PMP sample mass, the Nano-mag 250 nm paramagnetic particles gives greatest frequency shifts, inferring greatest sensitivity in the linear region. Values of sensitivity (Hz/ $\mu\text{g}$ ) measured at  $1\mu\text{g}$  for each PMP are provided in table 1. From results presented in table 1 it is evident that the sensitivity in Hz/ $\mu\text{g}$  increases with a decrease in the diameter of the PMPs. For a given mass of particles, the smaller PMPs will have a greater packing density close to the reaction surface and consequently close to the coil. The flat spiral sensing coil produces an electromagnetic field that varies with distance from the coil surface and can be predicted by applying Biot-Savart's law [6]. As a result, the change in inductance due to the smaller PMPs, which are more densely packed at the surface, will be greater.

#### 4.3 Monolayer susceptibility

To predict which PMP will provide optimum performance during assay measurement in respect of the properties of the PMP, the response of the system to a monolayer of PMPs corresponding to the area of the reaction surface was determined. From figure 5 at low mass values the relationship between frequency change and sample mass is linear. Consequently, the frequency change caused by a monolayer coverage of the detection region ( $\Delta f_{\text{monolayer}}$ ) can be calculated using equation (6), where S is the detection sensitivity (Hz/ $\mu\text{g}$ ).

$$\Delta f_{\text{monolayer}} = n_{\text{pmp}} N_{\text{pmp}} S \quad (6)$$

Figure 6 shows the frequency change for a monolayer for each type of PMP, calculated from equation (6) and figure 5. In addition, in figure 6, values of mass susceptibility of a monolayer for each type of PMP, calculated from equation 5 are presented. The least squares fit line, with a squared multiple correlation coefficient ( $R^2$ ) of 0.9174, illustrates an approximately linear relationship between the frequency change that would be generated when using a particular PMP in a RCM and the mass susceptibility of a monolayer of the PMP. This indicates that the monolayer mass susceptibility parameter provides a useful mechanism for determining PMPs that will provide optimum sensitivity when used as a label in a MIA. As illustrated in figure 6, Estapor 0.75 $\mu\text{m}$  PMPs give the highest frequency shift of 667 Hz and have the greatest magnetic susceptibility of  $1.11 \times 10^{-6}$ . The smallest 250 nm PMPs give the lowest frequency shift of 200 Hz.

Equation 5 also provides a mechanism for predicting suitability for use in MIA of novel PMPs. For example, an investigation into the use of 12 nm gold-coated iron nano-particles as magnetic labels [9] has revealed that the nano-particles offered an order of magnitude higher magnetic susceptibility and approximately five times higher percentage of magnetic material content than that of the Dynal 2.8  $\mu\text{m}$  particles. According to equation 5 this type of particle would potentially offer an attractive alternative to existing iron-oxide based particles.

In addition to the magnetic properties other factors are also critical when determining which PMPs should be used to provide a sensitive and robust magneto-immunoassay. The surface chemistry is important to ensure effective immobilisation of proteins. Both the density and orientation of binding molecules such as antibodies needed to be optimised for each assay. Other factors relating to the physical properties of the particles will influence their performance. For example the distribution of size and shape will influence the degree of binding taking place in the assay and consequently the response of the coil. Particular problems are encountered if ferromagnetic materials or particles with high hydrophobic surfaces are used, as these can lead to the formation of aggregates during the coating of the PMP surfaces.

## **5. Conclusion.**

The magnetic properties of PMPs which are relevant for their use in a magneto-immunoassay from a range of manufacturers have been compared. Magnetisation curves have been obtained using a vibrating sample magnetometer and a prediction of sample response in an assay has been performed using a magnetometer based on a resonant, planar, spiral coil and phase locked loop based detection circuitry. The results demonstrate that for optimum sensitivity of the system to a monolayer of PMPs, the mass susceptibility of the monolayer of PMPs must be maximised. This implies that the PMP mass, mass susceptibility and the percentage of magnetic material within the PMP should be as large as possible, whereas the cross sectional area of the PMP should be minimised. From the five commercially available PMPs evaluated in this study, the PMP providing the best performance was the 0.75 $\mu\text{m}$  PMP manufactured by Estapor.

## **Acknowledgments**

The authors gratefully acknowledge the support of Randox Laboratories for support of this work.

## **References**

1. .Luppa, P., Sokoll, L. J., Chan, D. W., 'Immunoassays - principles and applications to clinical chemistry', Clinica Chimica Acta, 2001, 314 pp1-26.

2. Hawkanes, B.I., Kvam, C., 'Application of magnetic beads in bioassays' *Biotechnology*, 1993, 11, pp60-63.
3. Thiel, A., Scaffold, A., Radbruch, A., 'Immunomagnetic cell sorting-pushing the limits.', *Immunotechnology*, 1998, 4, pp89-96.
4. Dogeigne, C., Lejeune R., 'Chemiluminescence as a diagnostic tool – a review' *Talanta*, 2000, 51, pp415-439
5. Kiely, J., Hawkins, P, Wraith, P., Luxton, R., 'Paramagnetic particle detection for use with an immunoassay based biosensor', *IEE Journal of Science, measurement and technology*, 2007, 1 (5), pp 270-275.
6. Luxton, R., Jasavant, Badesha., Janice Kiely., Hawkins, P. 'The use of external magnetic fields to reduce reaction times in an immunoassay using micrometer-sized paramagnetic particles (Magneto-immunoassay)', 2004, *Analytical Chemistry* 76 (6), pp1715-1719
7. G. M. Brett, S. J. Chambers, L. Huang, M. R. A. Morgan, 'Design development of immunoassays for detection of proteins', *Food Control*, 1999, 10 (6), pp401-406.
8. Richardson, J., Hill, A., Luxton, R., Hawkins, P., 'A novel measuring system for the determination of paramagnetic particle labels for the use in magneto-immunoassays', *Biosensors & Bioelectronics*, 2001, 16, pp1127-1132
9. Carpenter, E.E., 'Iron nanoparticles as potential magnetic carriers', *Journal of Magnetism and magnetic Materials*, 2004, 225, pp17-20.

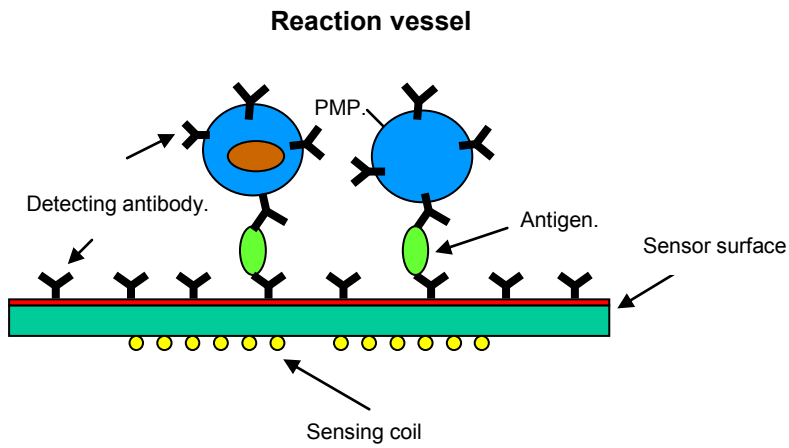


Fig. 1: Diagram of a sandwich magneto-immunoassay (MIA).

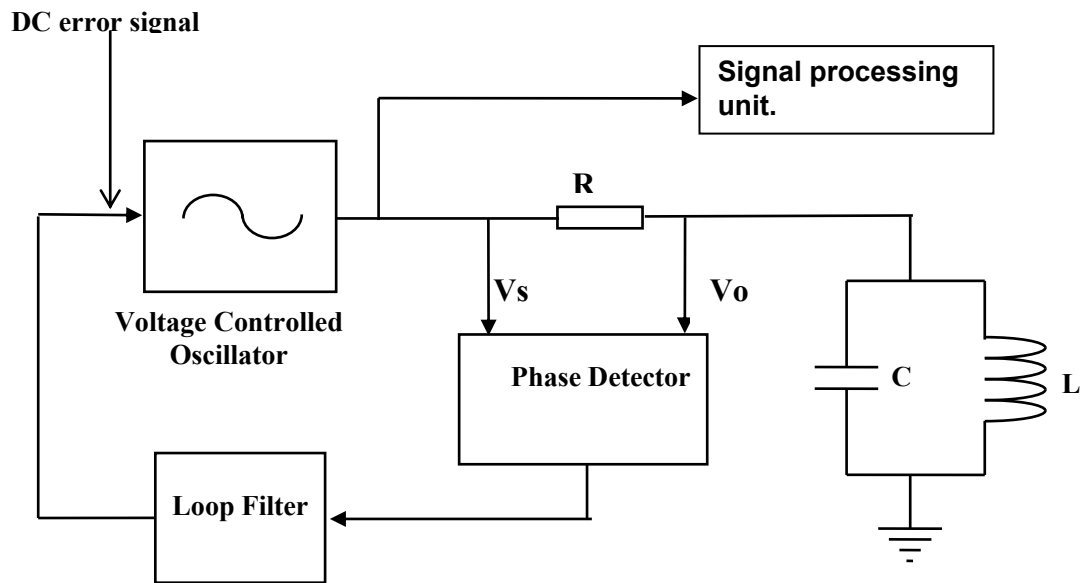


Fig. 2: Phase lock loop detection circuit.

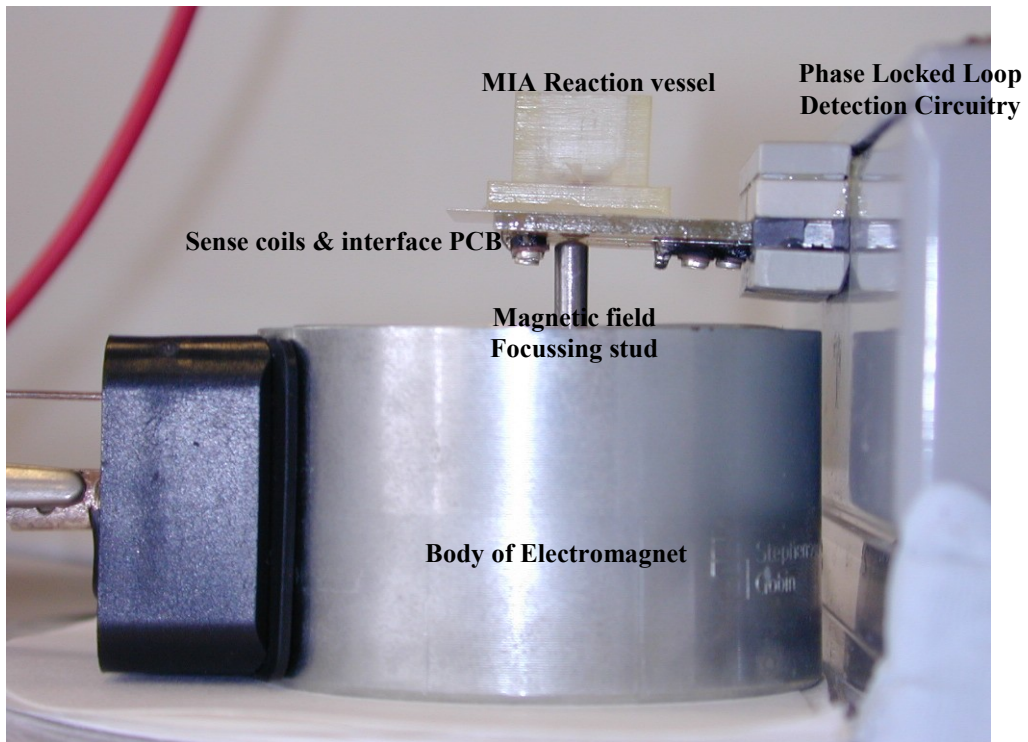


Figure 3: 35 MHz resonant coil magnetometer with detection coil interface PCB, electromagnet and reaction vessel.

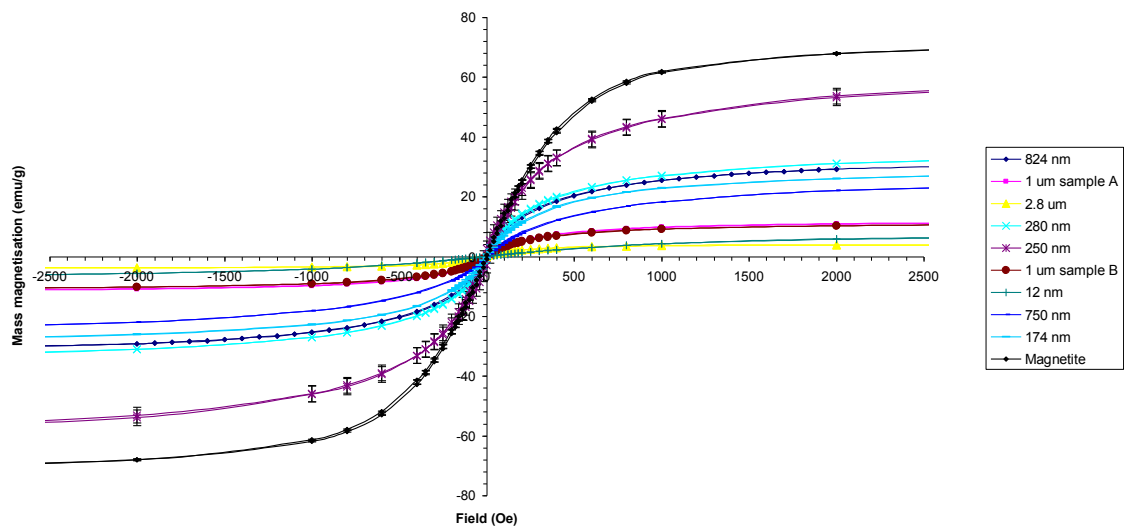


Figure 4: VSM magnetisation curves (magnetisation vs magnetic field strength) at 300 K in the field range  $\pm 6000$  Oe for PMPs of different size and manufacturer

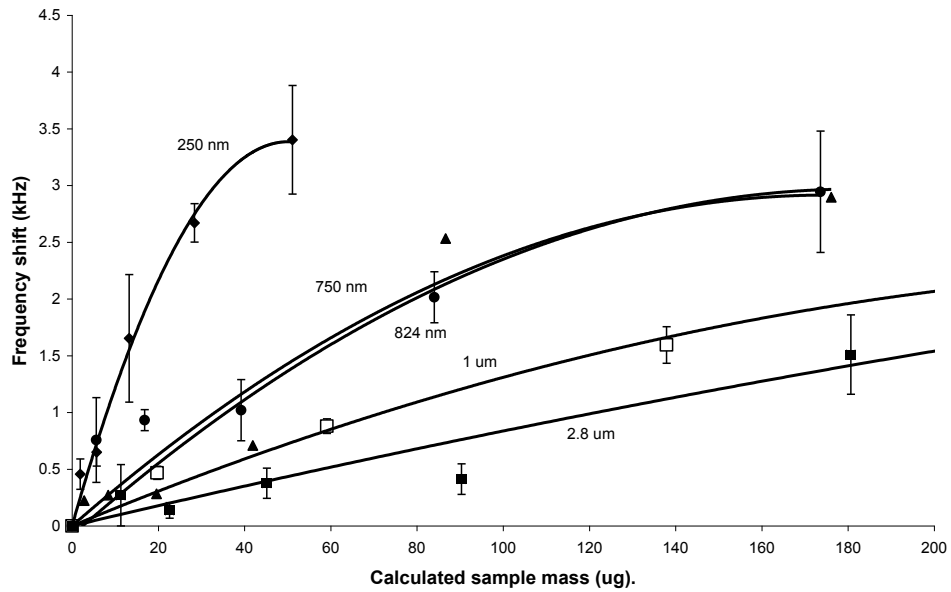


Figure 5: RCM's Average frequency change  $\Delta f$  dependence on PMP sample mass and type ( $n = 3$ ).

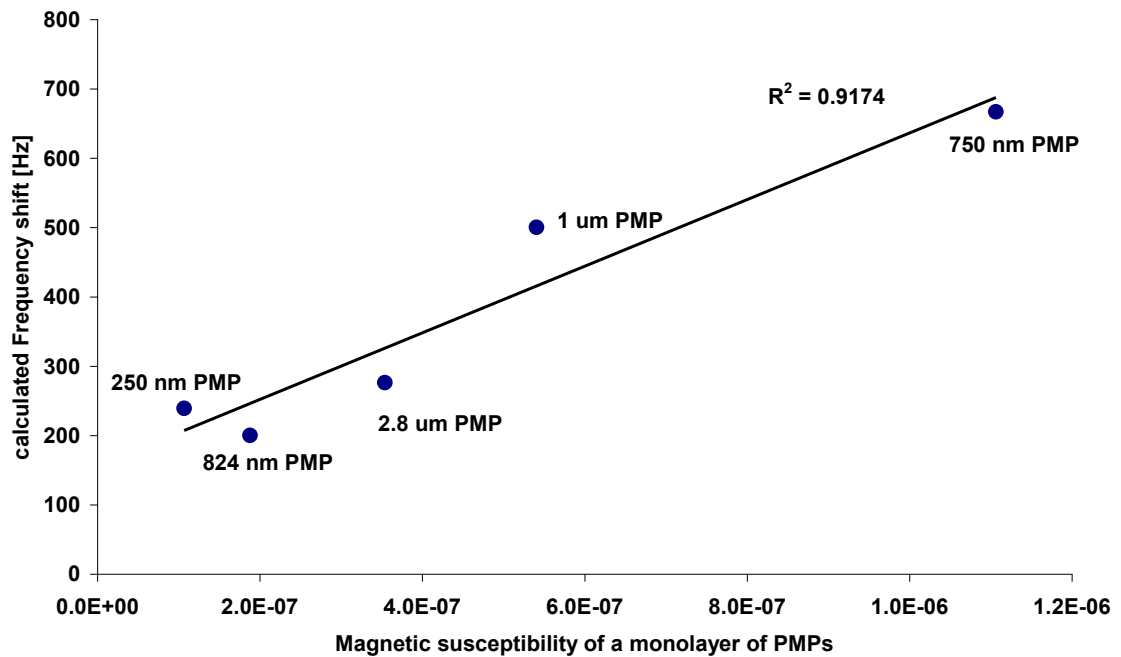


Figure 6: Calculated coil's frequency shift (Hz) versus mass susceptibility of a monolayer (emu/Oe) of selected paramagnetic particles.

<b>PMP diameter (µm)</b>	<b>Manufacturer</b>	<b>% Magnetic material content</b>	<b>Numbers of PMPs / mL in 1% stock conc.</b>	<b>Mass susceptibility at 300 K emu/Oe.g</b>	<b>Saturation magnetisation at 300 K emu/g</b>	<b>Sensitivity Hz/µg</b>
0.25	Nano-mag	80	$4.9 \times 10^{11}$	$1.52 \times 10^{-1}$	60	125
0.75	Estapor	48.5	$3.09 \times 10^9$	$5.72 \times 10^{-2}$	26.5	33
0.824	Seradyn	40	$1.01 \times 10^{10}$	$8.62 \times 10^{-2}$	33.2	34
1	Dynal	37	$4.64 \times 10^9$	$4.42 \times 10^{-2}$	11.5	16
2.8	Dynal	17	$6.8 \times 10^9$	$2.37 \times 10^{-2}$	37.2	9

Table 1 – PMP diameter and % magnetic content from manufacturer's data sheets and number of PMPs in 1% stock solution, mass susceptibility, saturation magnetization and sensitivity values for PMPs from a range of manufacturers